Supplementary Materials for

Enhanced efficiency and environmental stability of planar perovskite solar cells by suppressing photocatalytic decomposition

Peng Zhang[1], Jiang Wu[2], Yafei Wang[1], Hojjatollah Sarvari[3], Detao Liu[1], Zhi David Chen[1,3,*] & Shibin Li[1,*]

1 School of Optoelectronic Information, University of Electronic Science and Technology of China, Chengdu 610054, China.

2 Department of Electronic and Electrical Engineering, University College London, Torrington Place, London WC1E7JE, UK.

3 Department of Electrical & Computer Engineering and Center for Nanoscale Science & Engineering, University of Kentucky, Lexington, Kentucky 40506, USA.

[*] Address correspondence to Shibin Li, shibinli@uestc.edu.cn; Zhi David Chen, zhichen@engr.uky.edu

This file includes:

- Figure S1. The transmittance of Al-ZnO and RF-ZnO films;
- Figure S2. The J-V curve and EQE spectra of S-ZnO device;
- Figure S3. The J-V curves of best performing PSC based on Al-ZnO measured by forward and reverse scans;
- Figure S4. The steady state photocurrent output of the best performing PSC based on Al-ZnO;
- Figure S5. The evolution of S-ZnO device photovoltaic parameters over time;
- Figure S6. The absorption evolution of $MAPbI_3$ on S-ZnO and photos of the perovskite film;
- Figure S7. The evolution of ideal factor and reverse saturated current density over time;
- Figure S8. The SEM of surface and cross section of $MAPbI_3$ on S-ZnO;
- Figure S9. The V_{TFL} of the electron-only device based on S-ZnO;
- Figure S10. The PL and TRPL spectra of perovskite on Al-ZnO, RF-ZnO and S-ZnO;
- Table S1. Detail photovoltaic data of Al-ZnO, RF-ZnO and S-ZnO devices before and after aging.

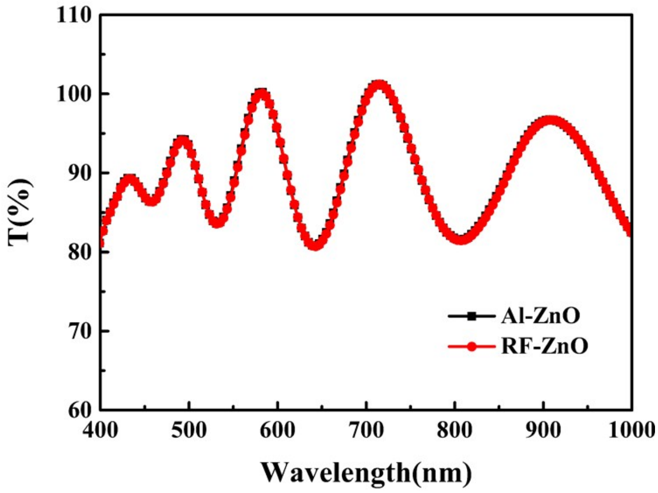

Figure S1. The transmittance of Al-ZnO and RF-ZnO. We can see that the transmittance of ZnO film with Al interlayer has no obvious difference with bare ZnO, and this will minimize the incident light power loss.

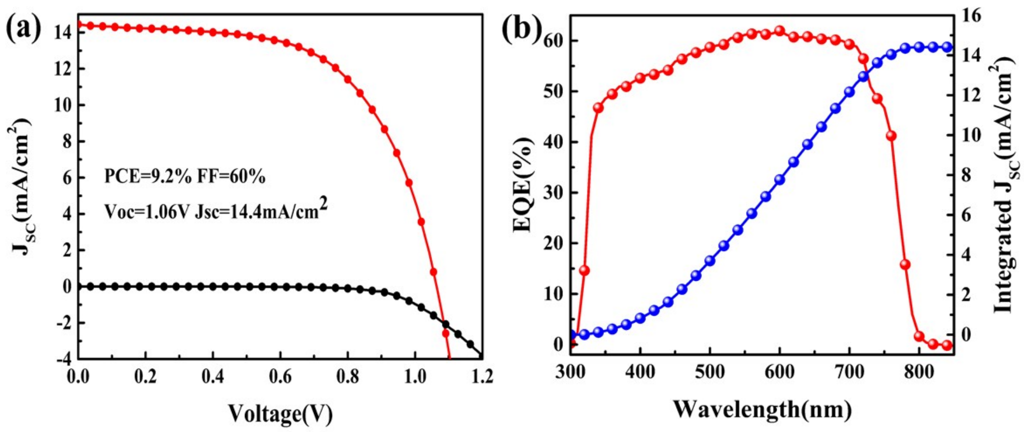

Figure S2. (a)The J-V curve and photovoltaic parameters of the S-ZnO control device. Compared with RF-ZnO and Al-ZnO devices, the performance of S-ZnO control device shows a stark drop. This decrease is mainly from the severely surface recombination. (b). The EQE spectra of PSC based on S-ZnO. The Jsc calculated from EQE data is 14.4 mA/cm^2, which is consisted with the Jsc from the J-V test. The EQE spectra show a response in range of 350 nm - 700 nm. However, compared with the samples based on Al-ZnO and RF-ZnO, the whole spectrum response is significantly decreased.

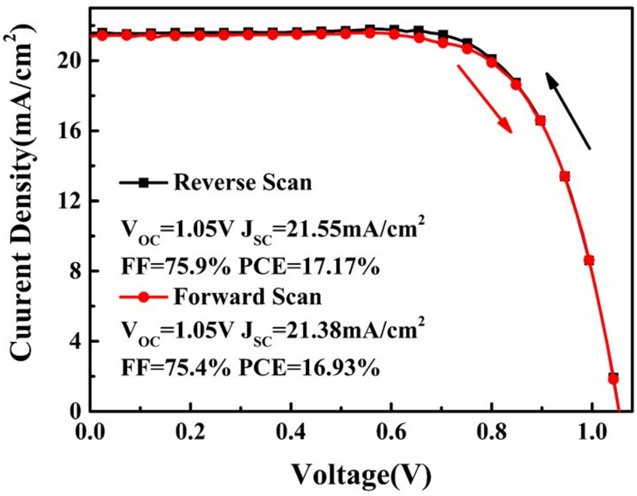

Figure S3. The J-V curves of best performance PSC based on Al-ZnO measured by forward and reverse scans. As can be seen, the Jsc, FF and PCE obtained from forward scan slightly decreased and small hysteresis between two scan directions was observed.

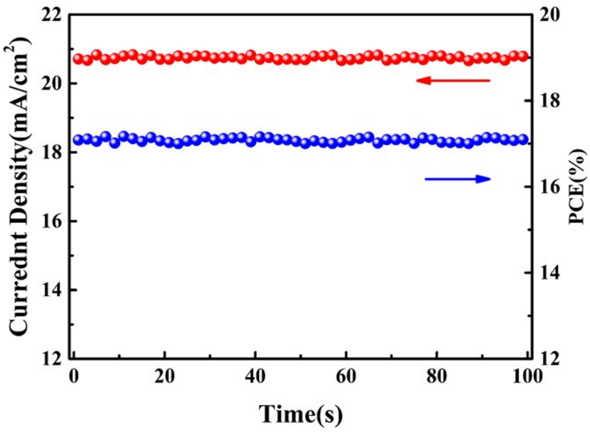

Figure S4. The steady state photocurrent output of the best performing PSC based on Al-ZnO, measured at the maximum power point (0.824V). The stable photocurrent obtained is 20.8 mA/cm^2, and the stable PCE is 17.05%.

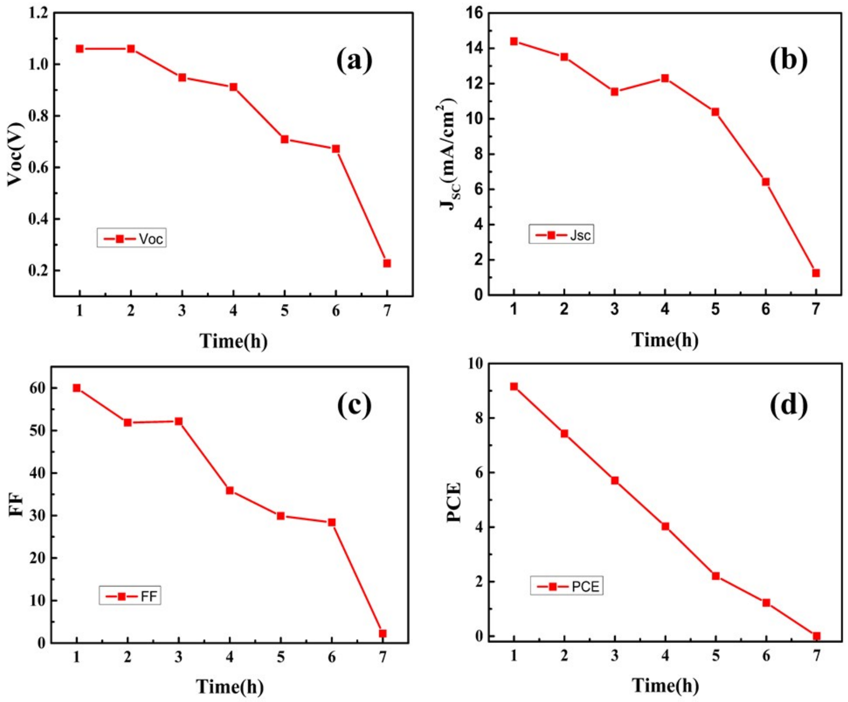

Figure S5. The regression of S-ZnO device photovoltaic parameters over time. All the photovoltaic parameters of S-ZnO control device decrease immediately after the start of the aging process. Complete device failure is observed in just 7 hours of aging test.

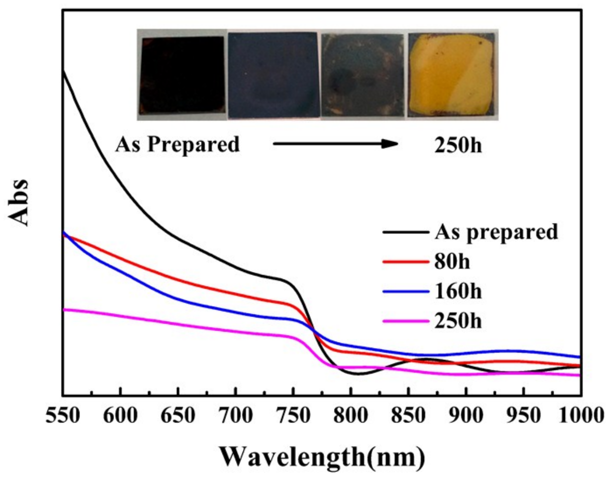

Figure S6. The UV-VIS absorption of $MAPbI_3$ on S-ZnO, and inset photos of the film aging over time. The missing absorption corresponding to PbI_2 before aging demonstrates the full conversion of $MAPbI_3$ precursor. As the increase of aging time, the background absorption increase over time during aging process because the decomposition of $MAPbI_3$. At the same time, the appearance of $MAPbI_3$ film changed obviously, the color of $MAPbI_3$ film change from dark brown to yellow during aging process, like the photos shown in inset.

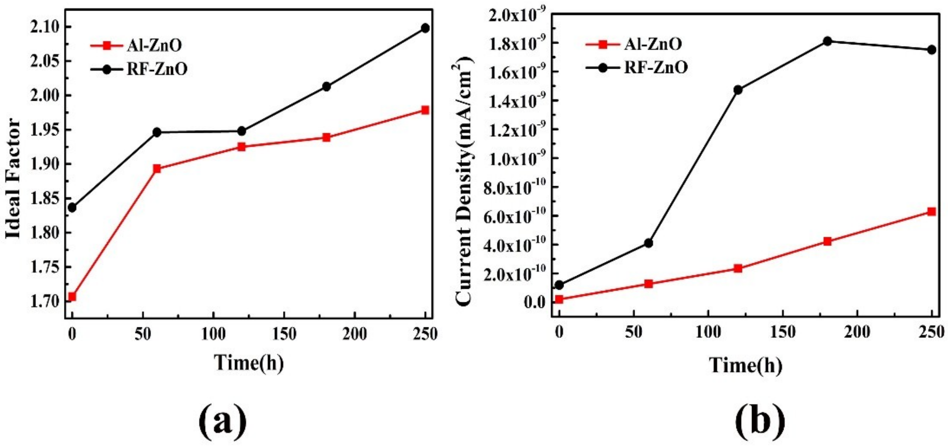

Figure S7. The evolution of ideal factor and reverse saturated current density over time.

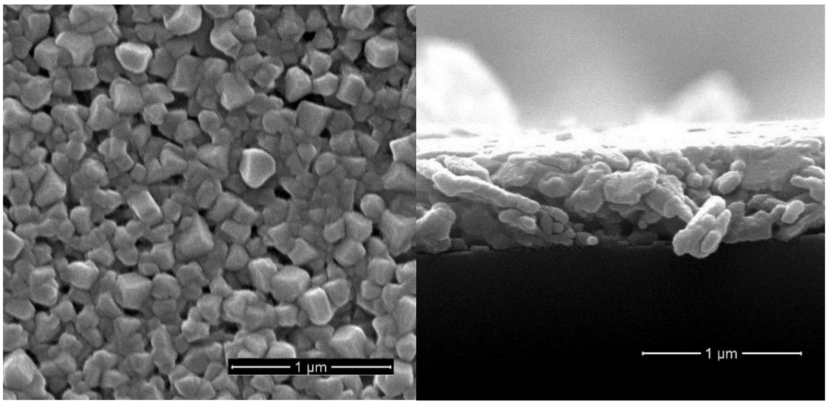

Figure S8. The SEM of surface and crosection morphology of $MAPbI_3$ on S-ZnO. As we can see, unlike dense and uniform film on RF-ZnO and Al-ZnO, there are many holes in $MAPbI_3$ film on S-ZnO. The holes increase the chance of direct contact between ETM and HTM, which will lead the short circuit of the device. And at the same time, the size of $MAPbI_3$ grain decrease. Small $MAPbI_3$ grain will increase the series resistance, which is unfavorable to PSCs.

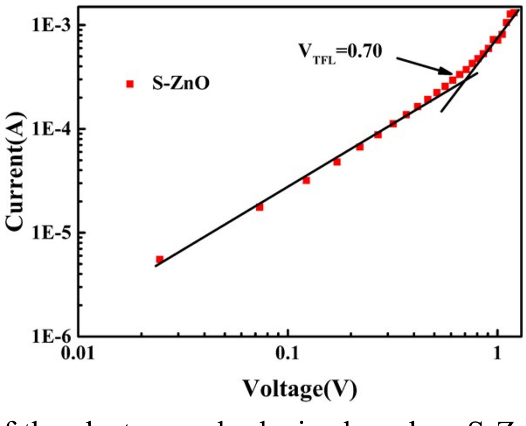

Figure S9. The V_{TFL} of the electron-only device based on S-ZnO. Higher V_{TFL} means the high trap density in $MAPbI_3$ film.

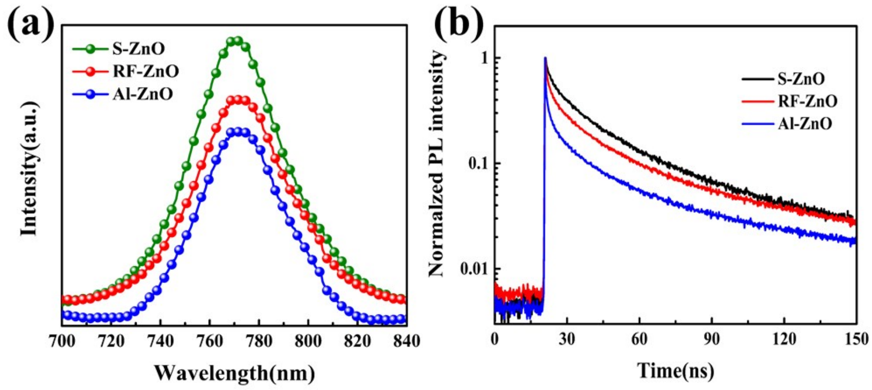

Figure S10. (a) The photoluminescence (PL) spectra and (b) the time-resolved photoluminescence (TRPL) spectra of perovskite films on Al-ZnO, RF-ZnO and S-ZnO. As can be seen, the perovskite film on Al-ZnO shows the weakest spectra intensity and shortest decay time, which mean the quality of perovskite film and electron extraction efficiency were improved by the AlO_x modification.

Table S1. Detail photovoltaic data of Al-ZnO, RF-ZnO and S-ZnO devices before and after aging.

	Before Aging				After Aging			
	PCE	Voc(V)	Jsc(mA/cm^2)	FF	PCE	Voc(V)	Jsc(mA/cm^2)	FF
S-ZnO	9.2%	1.06	14.4	60%	0.0064%	0.23	1.25	2.24%
RF-ZnO	14.62%	1.05	20.4	68.25%	7.07%	1.00	14.9	47.43%
Al-ZnO	17.17%	1.053	21.55	75.91%	15.03%	1.034	21.15	68.72%